Change in types of neuronal excitability via bifurcation control

Yong Xie,[1,2,*] Kazuyuki Aihara,[2] and Yan Mei Kang[3]
[1]*MOE Key Laboratory for Strength and Vibration, School of Aerospace, Xi'an Jiaotong University, Xi'an 710049, People's Republic of China*
[2]*Institute of Industrial Science, The University of Tokyo, 4-6-1 Komaba, Meguro-ku, Tokyo 153-8555, Japan*
[3]*School of Science, Xi'an Jiaotong University, Xi'an 710049, People's Republic of China*
(Received 18 October 2007; revised manuscript received 6 December 2007; published 27 February 2008)

This paper proposes an approach to changing the types of neuronal excitability via bifurcation control. A washout filter-aided dynamic feedback controller is introduced to bifurcation dynamics of a two-dimensional Hindmarsh-Rose type model neuron, which shows a saddle-node on invariant circle (SNIC) bifurcation from quiescence to periodic spiking and then exhibits type-I excitability. At first, a Hopf bifurcation is created at a desired parameter value before the SNIC bifurcation occurs, and then the criticality of the created Hopf bifurcation is regulated by choosing appropriate values of the controller parameters. In this manner, the model neuron starts to show type-II excitability. Therefore the type of neuronal excitability is transformed from type-I excitability to type-II excitability for the model neuron via the washout filter-aided dynamic feedback controller. In such a controller, the linear control gain is determined by the two basic critical conditions for the Hopf bifurcation, i.e., the eigenvalue assignment and the transversality condition. We apply the center manifold and normal form theory to deduce a closed-form analytic expression for the bifurcation stability coefficient, which is a function with respect to the nonlinear control gain. A suitable nonlinear control gain is chosen to make the bifurcation stability coefficient negative, and thus the criticality of the created Hopf bifurcation can be changed from subcritical to supercritical. In addition, the amplitude of the corresponding periodic solution can be also regulated by the nonlinear control gain.

DOI: 10.1103/PhysRevE.77.021917 PACS number(s): 87.19.L−, 05.45.−a, 07.05.Dz

I. INTRODUCTION

Spiking neurons are classified into two types, namely type-I excitability and type-II excitability according to the frequency response characteristics of a neuron to a constant current stimulation [1,2]. A neuron with type-I excitability is characterized by a continuous FI (the firing frequency versus the applied current) curve that shows oscillations starting with an arbitrarily low frequency. The firing frequency varies continuously from almost zero to a certain value with a wide dynamic range as the applied current changes. In contrast, a neuron with type-II excitability is characterized by a discontinuous FI curve with the oscillations starting with a nonzero frequency, and the response frequency range is narrow [1–4]. For a neuron with type-I excitability there is an apparent threshold for the appearance of spikes, while there is no true threshold for a neuron with type-II excitability, rigorously speaking [1,5]. Therefore there is a great difference in firing behavior between them. Despite a large number of biophysical mechanisms, there are only two major dynamical mechanisms underlying neuronal excitability observed frequently in nature because of the codimension one bifurcation, namely, the saddle-node on invariant circle (SNIC) bifurcation and the Hopf bifurcation (HB) [5–7]. In general, the former underlies type-I excitability, while the latter mediates type-II excitability. Here, the Hopf bifurcation can be either subcritical or supercritical.

Neuronal excitability is responsible for the translation of synaptic input to the particular output function of a given neuron, and directly attributable to the suite of ion channels inserted into the membrane of the cell as well as the biochemical properties and kinetics of those channels. Therefore changes in neuronal excitability may occur through a variety of means, including changes in passive membrane properties (capacitances and resistances) or changes in voltage-activated currents [8]. It is possible that mechanisms that alter neuronal excitability lead to a kind of plasticity in responses to synaptic stimulation, ultimately affecting processes such as learning and memory and other activity-dependent forms of neural plasticity [8]. As is known, normal aging subjects have difficulty learning hippocampus-dependent tasks. The pronounced decrease in neuronal excitability observed in hippocampal pyramidal neurons can be an important cause for the age-related learning impairment [9]. Actually, neuronal excitability plays a rather complicated role in neurophysiological activities, and maintenance of proper neuronal excitability is vital to nervous system function and normal behavior. On the other hand, activity-dependent changes in neuronal excitability and synaptic strength are thought to underlie memory encoding. Especially, in hippocampal CA1 neurons, small conductance Ca2+-activated K+ (SK) channels contribute to the afterhyperpolarization, affecting neuronal excitability [10]. Neurons are challenged with perturbations that can alter excitability, including changes in cell sizes, innervation, and synaptic input. In general, neurons have the ability to compensate for these types of perturbations and maintain appropriate levels of excitation [11]. Surprisingly, changes in neuronal excitability also can have a stabilizing influence on nervous system function [8]. Some neurons may respond to changes in synaptic input or endogenous activity by altering their excitability to maintain a given firing pattern or a firing rate. For

*yxie@mail.xjtu.edu.cn

example, a pacemaker neuron that experiences a decrease in synaptic drive may independently increase its own excitability by up-regulating depolarizing conductances in order to maintain a fixed level of firing output [8]. In this study, we change the types of neuronal excitability via bifurcation control, and expect that our control method can make neuronal excitability change from abnormal to normal under some situation and thus regulate abnormal firing behavior of neurons by a dynamic feedback controller.

Bifurcation control refers to the task of designing a controller to modify the bifurcation properties of a given nonlinear system, thereby achieving some desirable dynamical behavior [12]. The potential applications of bifurcation control have been widely reported in various fields, such as regulating human heart rhythms and neuronal firing behavior [13,14], controlling the high angle-of-attack flight dynamics [15], reducing vibration of hard drives [16], and designing an alert system for impending voltage collapse and catastrophe in power systems [17]. Generally, bifurcation control has many different types of tasks, such as delaying the onset of an inherent bifurcation, relocating existing bifurcation points, modifying the shape or type of a bifurcation solution, creating a desired type of bifurcation at preferable parameter values, stabilizing a bifurcated periodic solution or branch, and optimizing the system performance near a bifurcation point [12]. At present, representative approaches of bifurcation control include washout filter-aided dynamic feedback [18], linear or nonlinear state-feedback [19,20], harmonic balance approximation [21], and quadratic invariants in normal forms [22].

As mentioned above, changes in types of neuronal excitability actually imply changes in dynamical mechanisms underlying neuronal excitability, that is, variation in types of bifurcation. Specifically, we convert type-I excitability into type-II excitability by a washout filter-aided dynamic feedback controller. In other words, such a controller is adopted for the creation of a Hopf bifurcation before the occurrence of a SNIC bifurcation. It is known that static state feedback does not apply to problems where the dynamics and the targeted operating point are uncertain [23]. Moreover, static state feedback changes the operating conditions of the open-loop system. This may result in waste of control energy and also induce degradation of system performance. Fortunately, washout filters can overcome these difficulties. In fact, a washout filter is a high pass filter that washes out steady state inputs, while passing transient inputs [20]. The use of washout filters ensures that all the equilibrium points of an open-loop system are preserved in the closed-loop system; namely, their locations are not changed. Recently, it has been reported that the washout filters can be applied for the creation of Hopf bifurcations in continuous-time systems [24]. In addition, washout filters facilitate automatic following of targeted operating points, which results in vanishing control energy once stabilization is achieved and a steady state is reached.

In this paper, a two-dimensional Hindmarsh-Rose (HR) type model [4] is utilized as a model neuron because it not only can exhibit type-I excitability under appropriate values of parameters but also possesses a set of simple expression formulas. It is well-known that a Hopf bifurcation occurs with basic critical conditions, i.e., the eigenvalue assignment and the transversality condition [25,26]. Since such two basic critical conditions can be merged into a simple algebraic form, the implicit criterion is preferable for derivation of an analytical solution for the control gains without direct analytical computation of the eigenvalues as functions of the control gains, which is sometimes considerably difficult or even impossible for high-dimensional systems [24,27]. Through a coordinate transformation we convert the closed-loop system into a canonical form and then obtain a closed-form analytic expression for the bifurcation stability coefficient by application of the center manifold and normal form theory.

The paper proceeds as follows. In Sec. II, we describe the two-dimensional HR neuronal model and describe its dynamics. For such a model neuron a Hopf bifurcation is created via a washout filter-aided controller at a desired parameter value according to the two basic critical conditions, thus transformation of type-I excitability into type-II excitability is achieved in Sec. III. In Sec. IV, we derive a closed-form analytic expression for the bifurcation stability coefficient as a function of control gains, and then change the created Hopf bifurcation from subcritical to supercritical. Some conclusions are drawn in Sec. V.

II. TWO-DIMENSIONAL HINDMARSH-ROSE TYPE MODEL AND ITS DYNAMICS

The two-dimensional HR type model was analyzed by Tsuji *et al.* [4] as a neuronal model. It is described by the following equations:

$$\frac{dx}{dt} = c\left(x - \frac{x^3}{3} - y + z\right),$$

$$\frac{dy}{dt} = \frac{x^2 + dx - by + a}{c},$$

where x and y denote the cell membrane potential and a recovery variable, respectively. a, b, c, d, and z are parameters. In particular, z represents the external stimulus. Bifurcation behavior of this model has been explored in detail [4].

Under a set of parameter values, namely, $a=0.42$, $b=1.0$, $c=3.0$, and $d=1.8$, the neuron exhibits type-I excitability as the external stimulus z changes, as shown in Fig. 1. Figures 1(a) and 1(b) correspond to the bifurcation diagram and the firing frequency versus the applied current, respectively. There is a SNIC bifurcation at $z=0.3463$, where the neuron model generates the SNIC bifurcation from quiescence to firing. A subcritical Hopf bifurcation occurs at $z=2.3420$. Note that the firing frequency varies continuously from almost zero. All bifurcation diagrams in this paper were produced using the software package XPPAUT, which is software for the analysis and simulation of dynamic systems and can

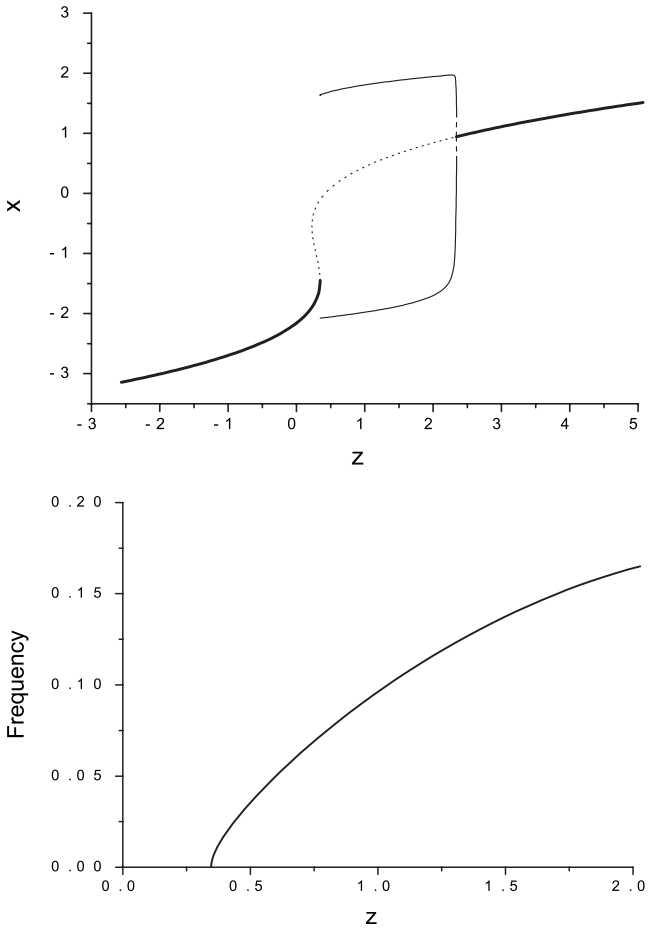

FIG. 1. Type-I excitability. (a) The bifurcation diagram of the HR type model with type-I excitability. The thick solid lines denote stable steady states, while the dotted line shows unstable equilibrium points. The thin lines represent the maximum and minimum values of stable limit cycles, and the dashed lines are the maximum and minimum values of unstable limit cycles. The captions of all the other bifurcation diagrams in this paper are the same as this caption. (b) The firing frequency versus the applied current.

trace the steady states and periodic solutions irrespective of whether they are stable or unstable [28].

III. TRANSFORMATION OF TYPE-I EXCITABILITY INTO TYPE-II EXCITABILITY

In this section, we introduce a Hopf bifurcation at $z_0 = -0.5$ via a washout filter-aided dynamic feedback controller. This makes neuronal excitability change from type-I excitability into type-II excitability.

In continuous-time systems, the transfer function of a typical washout filter is given as follows [23]:

$$G(s) = \frac{y(s)}{x(s)} = \frac{s}{s + d_f} = 1 - \frac{d_f}{s + d_f},$$

where d_f is the reciprocal of the filter time constant which is positive for a stable filter and negative for an unstable filter. With the following notation,

$$w(s) = \frac{1}{s + d_f} x(s),$$

the equation of the state variable w of the filter can be written as

$$\frac{dw}{dt} = x - d_f w.$$

The benefits of applications of washout filters are to preserve the equilibrium structure of the open-loop system as well as to save control energy. Here, we only use one washout filter associated with membrane potential x. The membrane potential is chosen as an input to the washout filter because it can be readily measured, and the controller can be realized easily. The equations of the two-dimensional HR model with a dynamic feedback controller through a washout filter are given as follows:

$$\frac{dx}{dt} = c\left(x - \frac{x^3}{3} - y + z\right) + u,$$

$$\frac{dy}{dt} = \frac{x^2 + dx - by + a}{c},$$

$$\frac{dw}{dt} = x - d_f w,$$

$$u = g(v), \quad v = x - d_f w,$$

where $d_f > 0$ such that the washout filter is stable. In this paper, we set $d_f = 0.1$. v is the output function of the washout filter.

For the above closed-loop system, in addition to the creation of a Hopf bifurcation, our controller can be designed to control the criticality of the bifurcation as shown in the next section. It is well-known that only the quadratic and cubic terms in a nonlinear system generating a Hopf bifurcation influence the bifurcation stability coefficient [19,26]. In order to simplify the choice of control parameters, however, we represent our controller in the following simple form with only a linear term and a cubic term:

$$u = K_l(x - d_f w) + K_n(x - d_f w)^3.$$

Note that introduction of the washout filter to the two-dimensional HR model does not affect the equilibrium structure of the original system during a control process. As we shall see later, the linear control gain K_l determines two basic critical conditions, but has no effect on the criticality of the bifurcation because of no contribution to the bifurcation stability coefficient; the nonlinear control gain K_n, on the other hand, controls the criticality of the bifurcation, but has no influence on the locations of equilibrium points.

Suppose that a Hopf bifurcation is created at a desired parameter value $z_0 = -0.5$ before the emergence of the SNIC bifurcation. For the closed-loop system it has only one equilibrium point at $z_0 = -0.5$, namely, $(x_0, y_0, w_0) = (x_0, y_0, x_0/d_f) = (-2.481\,04, 2.109\,68, -24.8104)$. The Jacobian matrix of the closed-loop system is given as follows.

$$\begin{bmatrix} c(1-x^2)+K_l+3K_n(x-d_fw)^2 & -c & -K_ld_f-3K_n(x-d_fw)^2d_f \\ \frac{2x+d}{c} & -\frac{b}{c} & 0 \\ 1 & 0 & -d_f \end{bmatrix}.$$

It is clear that the nonlinear control term has no influence on the Jacobian matrix at the equilibrium point. Thus the Jacobian matrix becomes

$$\begin{bmatrix} c(1-x^2)+K_l & -c & -K_ld_f \\ \frac{2x+d}{c} & -\frac{b}{c} & 0 \\ 1 & 0 & -d_f \end{bmatrix}.$$

The corresponding characteristic equation has the following form:

$$p_0\lambda^3+p_1\lambda^2+p_2\lambda+p_3=0,$$

where

$$p_0=1,$$

$$p_1=d_f+\frac{b}{c}-c+cx^2-K_l,$$

$$p_2=\frac{bd_f-bK_l}{c}-d_fc+d_fcx^2+2x+d-b+bx^2,$$

$$p_3=d_f(2x+d-b+bx^2).$$

If a Hopf bifurcation occurs, the Jacobian matrix of the closed-loop system must satisfy the basic critical conditions [25,26]. One is the eigenvalue assignment. Namely, the characteristic equation has a pair of pure imaginary eigenvalues $\lambda_1=\omega_0 i$ and $\lambda_2=\bar{\lambda}_1=-\omega_0 i$, and the other eigenvalues have negative real parts at $z_0=-0.5$. The other is the transversality condition. That is, the eigenvalues λ_1 and λ_2 cross the imaginary axis with some nonzero speed at the Hopf bifurcation point $(x_0,y_0,w_0;z_0)$. To avoid solving directly all eigenvalues, we employ a more convenient and efficient algorithm criterion for detecting the existence of Hopf bifurcations, which is on basis of the Routh-Hurwitz stability criterion and described by the coefficients of the characteristic equation instead of eigenvalues [27].

In this way, the eigenvalues assignment corresponds to the following conditions.

$$p_3>0,$$

$$\Delta_1=p_1>0,$$

$$\Delta_2=\begin{vmatrix} p_1 & p_0 \\ p_3 & p_2 \end{vmatrix}=0.$$

Substituting the parameter values and the location of the equilibrium point, we can get

$$p_3=0.199\,35>0,$$

$$K_l<15.900\,00,$$

$$K_l^2-26.620\,42K_l+169.856\,70=0.$$

There are two solutions for the above equation, namely, $K_l=16.012\,99$ and $10.607\,43$. Apparently, only $K_l=10.607\,43$ meets the eigenvalue assignment. Next, we examine if $K_l=10.607\,43$ satisfies the transversality condition, which is written as

$$\left.\frac{\partial\Delta_2}{\partial z}\right|=-62.035\,10+4.721\,79K_l\neq 0,$$

$$\text{namely } K_l\neq 13.138\,04.$$

Apparently, $K_l=10.607\,43$ satisfies the transversality condition. As a result, we take $K_l=10.607\,43$ according to the two basic critical conditions for the occurrence of the Hopf bifurcation. For a while, let $K_n=0$, then the bifurcation diagram of the closed-loop system is shown in Fig. 2(a). As expected, a Hopf bifurcation is created at $z_0=-0.5$. At the same time, the right Hopf bifurcation is moved to $z=9.656$. Notice that the created Hopf bifurcation here is subcritcial. Figure 2(b) shows the firing frequency versus the applied current, which starts with a nonzero frequency. Thus we have made the neuronal excitability change from type-I excitability to type-II excitability.

IV. CONTROL OF CRITICALITY OF HOPF BIFURCATION

Since the created Hopf bifurcation is subcritical at $z_0=-0.5$, there is a bistable range in which the neuron exhibits either quiescence or repetitive firing (periodic spiking). This results in the occurrence of jump behavior between quiescence and repetitive firing. We can control the criticality of the created Hopf bifurcation by the nonlinear control term.

At a small neighborhood of a Hopf bifurcation point the bifurcated periodic solution of the limit cycle has the amplitude of $O(\varepsilon)$, here $\varepsilon=\sqrt{|z-z_0|}$. The asymptotic stability of such a periodic solution is governed by one characteristic exponent given by a real smooth even function $\beta(\varepsilon)=\beta_2\varepsilon^2+\beta_4\varepsilon^4+\cdots$. If $\beta(\varepsilon)<0$, the periodic solution is asymptotically stable, otherwise it is unstable. From the expression of

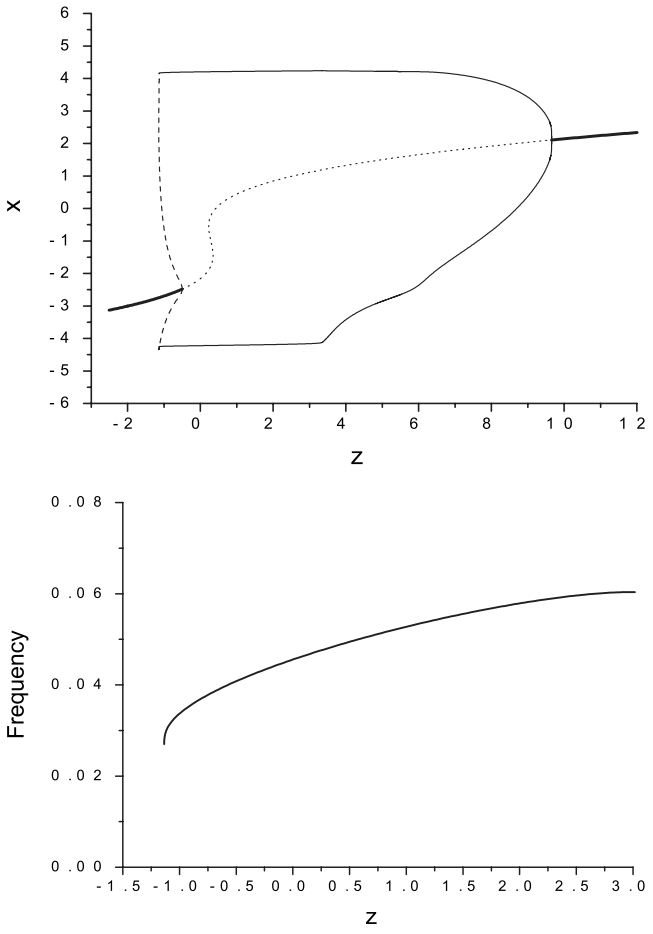

FIG. 2. Type-II excitability. (a) The bifurcation diagram of the closed-loop system with only the linear control term $K_l = 10.607\,43$. (b) The firing frequency versus the applied current.

$\beta(\varepsilon)$, typically, it can be seen that the local stability of the bifurcated periodic solution, namely, the criticality of the bifurcation, is determined by the sign of β_2, which is called the bifurcation stability coefficient. In what follows, we apply the center manifold and normal form theory to derive the closed-form analytic expression for β_2.

As seen above, after determining the linear control gain $K_l = 10.607\,43$ according to the two basic critical conditions for the Hopf bifurcation, the Jacobian matrix of the closed-loop system becomes a constant matrix. Therefore we can numerically compute all eigenvalues of the matrix and their corresponding eigenvectors. In fact, this is a necessary step in deriving the analytic expression for β_2 with respect to K_n in order to employ the center manifold and normal form theory.

The constant matrix is

$$\begin{bmatrix} -4.859\,23 & -3.0 & -1.060\,74 \\ -1.054\,03 & -0.333\,33 & 0.0 \\ 1.0 & 0.0 & -0.1 \end{bmatrix}.$$

The eigenvalues and their corresponding eigenvectors are

$$\lambda_1 = -1.162\,41 \times 10^{-10} + 0.194\,08i,$$

$$\lambda_2 = -1.162\,41 \times 10^{-10} - 0.194\,08i,$$

$$\lambda_3 = -5.292\,56,$$

and

$$v_1 = \begin{bmatrix} 0.084\,41 + 0.163\,81i \\ -0.424\,57 - 0.270\,80i \\ 0.844\,07 \end{bmatrix}, \quad v_2 = \bar{v}_1,$$

$$v_3 = \begin{bmatrix} -0.961\,25 \\ -0.204\,31 \\ 0.185\,12 \end{bmatrix}.$$

Here, i is the imaginary unit. Due to very small real parts of λ_1 and λ_2, the matrix can be considered to have a pair of pure imaginary eigenvalues. Another is a negative eigenvalue. For notational simplicity, let $\omega_0 = \mathrm{Im}(\lambda_1) = 0.194\,08$ and $M = \lambda_3 = -5.292\,56$. We construct a matrix P as follows:

$$P = [\mathrm{Re}(v_1), -\mathrm{Im}(v_1), v_3].$$

Here, Re and Im mean extracting the real part and the imaginary part of a complex-valued expression, respectively.

That is

$$P = \begin{bmatrix} 0.084\,41 & -0.163\,81 & -0.961\,24 \\ -0.424\,57 & 0.270\,80 & -0.204\,30 \\ 0.844\,07 & 0.0 & 0.185\,12 \end{bmatrix}.$$

Taking the following coordinate transformation,

$$\begin{bmatrix} x \\ y \\ w \end{bmatrix} = \begin{bmatrix} x_0 \\ y_0 \\ w_0 \end{bmatrix} + P \begin{bmatrix} X \\ Y \\ W \end{bmatrix},$$

we can obtain

$$\begin{bmatrix} x \\ y \\ w \end{bmatrix} = \begin{bmatrix} -2.481\,04 + 0.084\,41X - 0.163\,81Y - 0.961\,24W \\ 2.109\,68 - 0.424\,57X + 0.270\,80Y - 0.204\,30W \\ -24.810\,39 + 0.844\,07X + 01.851\,2W \end{bmatrix}.$$

Substituting the coordinate transformation into the closed-loop system, and then making the following transformation, we can get a system under a new coordinate system as follows:

$$\begin{bmatrix} \frac{dX}{dt} \\ \frac{dY}{dt} \\ \frac{dW}{dt} \end{bmatrix} = P^{-1} \begin{bmatrix} \frac{dx}{dt} \\ \frac{dy}{dt} \\ \frac{dw}{dt} \end{bmatrix} = \begin{bmatrix} F^1(X,Y,W) \\ F^2(X,Y,W) \\ F^3(X,Y,W) \end{bmatrix},$$

where P^{-1} is the following inverse matrix of P:

$$P^{-1} = \begin{bmatrix} 0.209\,47 & 0.126\,71 & 1.227\,53 \\ -0.392\,15 & 3.455\,58 & 1.777\,37 \\ -0.955\,09 & -0.577\,77 & -0.195\,11 \end{bmatrix}.$$

At $(X,Y,W)=(0,0,0)$ the Jacobian matrix of the new system is

$$\begin{bmatrix} -1.0\times10^{-10} & -0.194\,08 & 3.0\times10^{-9} \\ 0.194\,08 & 0.0 & -1.0\times10^{-9} \\ 0.0 & 0.0 & -5.292\,56 \end{bmatrix}.$$

We can regard the Jacobian matrix as the following matrix of the real canonical form by ignoring very small entries,

$$\begin{bmatrix} 0.0 & -0.194\,08 & 0.0 \\ 0.194\,08 & 0.0 & 0.0 \\ 0.0 & 0.0 & -5.292\,56 \end{bmatrix}.$$

As a result, the Jacobian matrix of the new system has the following property:

$$\begin{bmatrix} \frac{\partial F^1}{\partial X} & \frac{\partial F^1}{\partial Y} & \frac{\partial F^1}{\partial W} \\ \frac{\partial F^2}{\partial X} & \frac{\partial F^2}{\partial Y} & \frac{\partial F^2}{\partial W} \\ \frac{\partial F^3}{\partial X} & \frac{\partial F^3}{\partial Y} & \frac{\partial F^3}{\partial W} \end{bmatrix}_{(0,0,0)} = \begin{bmatrix} 0 & -\omega_0 & 0 \\ \omega_0 & 0 & 0 \\ 0 & 0 & M \end{bmatrix}.$$

Here, we can apply the center manifold and normal form theory to derive the analytic expression for the bifurcation stability coefficient β_2. In fact, by following the procedures provided in [29], the bifurcation stability coefficient has a unified expression, regardless of the detailed form of the transformed system with a real canonical form, as follows:

$$\beta_2(K_n) = 2\,\mathrm{Re}\left(\left[g_{20}(z_0)g_{11}(z_0) - 2|g_{11}(z_0)|^2 - \frac{1}{3}|g_{02}(z_0)|^2\right]\frac{i}{2\omega_0} + \frac{g_{21}(z_0,K_n)}{2}\right),$$

where

$$g_{20}(z_0) = \frac{1}{4}\left[\frac{\partial^2F^1}{\partial X^2} - \frac{\partial^2F^1}{\partial Y^2} + 2\frac{\partial^2F^2}{\partial X\,\partial Y} + i\left(\frac{\partial^2F^2}{\partial X^2} - \frac{\partial^2F^2}{\partial Y^2} - 2\frac{\partial^2F^1}{\partial X\,\partial Y}\right)\right],$$

$$g_{11}(z_0) = \frac{1}{4}\left[\frac{\partial^2F^1}{\partial X^2} + \frac{\partial^2F^1}{\partial Y^2} + i\left(\frac{\partial^2F^2}{\partial X^2} + \frac{\partial^2F^2}{\partial Y^2}\right)\right],$$

$$g_{02}(z_0) = \frac{1}{4}\left[\frac{\partial^2F^1}{\partial X^2} - \frac{\partial^2F^1}{\partial Y^2} - 2\frac{\partial^2F^2}{\partial X\,\partial Y} + i\left(\frac{\partial^2F^2}{\partial X^2} - \frac{\partial^2F^2}{\partial Y^2} + 2\frac{\partial^2F^1}{\partial X\,\partial Y}\right)\right],$$

$$g_{21}(z_0,K_n) = G_{21}(z_0,K_n) + 2G_{110}s_{11} + G_{101}s_{20},$$

$$G_{21}(z_0,K_n) = \frac{1}{8}\left[\frac{\partial^3F^1}{\partial X^3} + \frac{\partial^3F^1}{\partial X\,\partial Y^2} + \frac{\partial^3F^2}{\partial X^2\,\partial Y} + \frac{\partial^3F^2}{\partial Y^3} + i\left(\frac{\partial^3F^2}{\partial X^3} + \frac{\partial^3F^2}{\partial X\,\partial Y^2} - \frac{\partial^3F^1}{\partial X^2\,\partial Y} - \frac{\partial^2F^1}{\partial Y^3}\right)\right],$$

$$G_{110} = \frac{1}{2}\left[\frac{\partial^2F^1}{\partial X\,\partial W} + \frac{\partial^2F^2}{\partial Y\,\partial W} + i\left(\frac{\partial^2F^2}{\partial X\,\partial W} - \frac{\partial^2F^1}{\partial Y\,\partial W}\right)\right],$$

$$G_{101} = \frac{1}{2}\left[\frac{\partial^2F^1}{\partial X\,\partial W} - \frac{\partial^2F^2}{\partial Y\,\partial W} + i\left(\frac{\partial^2F^1}{\partial Y\,\partial W} + \frac{\partial^2F^2}{\partial X\,\partial W}\right)\right],$$

$$s_{11} = -h_{11}/M,$$

$$s_{20} = -h_{20}/(M - 2i\omega_0),$$

$$h_{11} = \frac{1}{4}\left(\frac{\partial^2F^3}{\partial X^2} + \frac{\partial^2F^3}{\partial Y^2}\right),$$

$$h_{20} = \frac{1}{4}\left(\frac{\partial^2F^3}{\partial X^2} - \frac{\partial^2F^3}{\partial Y^2} - 2i\frac{\partial^2F^3}{\partial X\,\partial Y}\right).$$

As above, all derivatives take their values at $(X,Y,W;z_0)=(0,0,0;-0.5)$. In this way, we obtain closed-form analytic expression for β_2 as follows:

$$\beta_2 = 0.225\,27\times10^{-1} + 2\,\mathrm{Re}(0.646\,45\times10^{-3}K_n + i0.345\,31\times10^{-3}K_n).$$

If K_n is a real number with $K_n<-17.423\,57$, $\beta_2<0$. As a consequence, $K_n<-17.423\,57$ ensures that the periodic solution bifurcated from the Hopf bifurcation is asymptotically stable, and then makes the Hopf bifurcation change from subcritical into supercritical. In contrast, if $K_n>-17.423\,57$, then $\beta_2>0$, and the created Hopf bifurcation is subcritical.

Let us investigate change of bifurcation behavior in the two cases of $K_n<-17.423\,57$ and $K_n>-17.423\,57$, respectively, to verify the accuracy of our analytic expression for β_2. Let $K_n=-20$ and -15.0, respectively. When $K_n=-20$, the bifurcation diagram is shown in Figs. 3(a) and 3(b). Figure 3(b) is an enlargement of Fig. 3(a) near the created Hopf bifurcation point. From Fig. 3(b), it is clear that the created Hopf bifurcation is supercritical. Thus we can make the created Hopf bifurcation supercritical via the nonlinear control term with $K_n=-20$. Figure 4 shows the bifurcation diagram with $K_n=-15.0$. Figure 4(b) is an enlargement of Fig. 4(a) near the created Hopf bifurcation point. Apparently, the created Hopf bifurcation is still subcritical. Further, it can be seen that there is a common characteristic between Figs. 3 and 4. Namely, the structure and locations of the equilibrium points are not changed. Also, the bifurcation points of the left (created) and the right Hopf bifurcations are not varied. The bifurcation value of the left HB is $z=-0.5$, while that of the right HB is $z=9.656$. In other words, the nonlinear control term only exerts an influence on the criticality of the bifurcations, namely, the bifurcation stability coefficient, but no effect on the structure and locations of the equilibrium points. Actually, these features can be seen from their calcu-

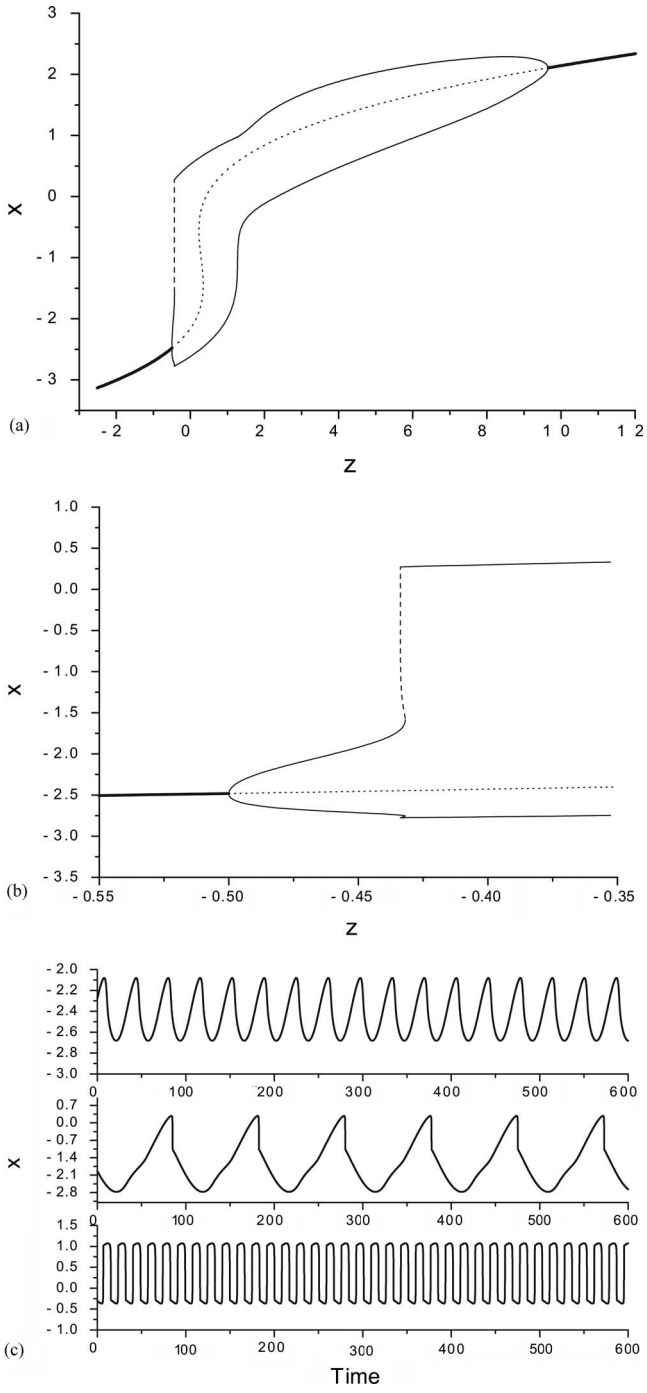

FIG. 3. The bifurcation diagram and time series of the closed-loop system with $K_l=10.607\,43$ and $K_n=-20.0$. (a) The bifurcation diagram, and (b) is an enlargement of (a) near the left Hopf bifurcation point. (c) Time series of the membrane potential correspond, respectively, to $z=-0.47$, -0.425, and 1.5 from top to bottom.

lation processes and expressions. When $z=-0.47$, -0.425, and 1.5, the neuron exhibits, respectively, a subthreshold oscillation, repetitive spiking, and a superthreshold oscillation with a small amplitude, as shown in Fig. 3(c).

By transforming the type of the Hopf bifurcation from subcritical to supercritical, the bistability near the created Hopf bifurcations is eliminated and thus the occurrence of jumping behavior between periodic spiking and quiescence of the closed-loop system under perturbation is prevented.

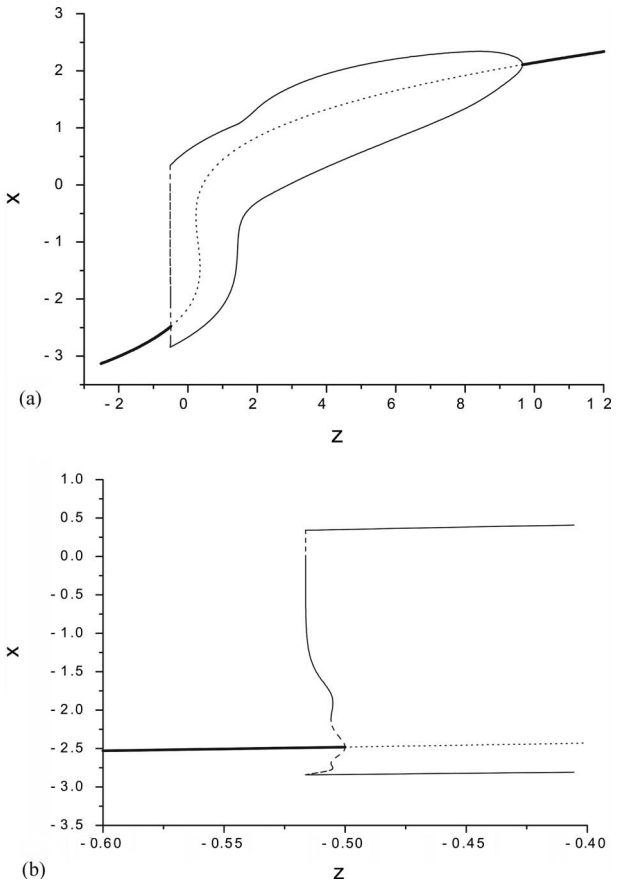

FIG. 4. The bifurcation diagram of the closed-loop system with $K_l=10.607\,43$ and $K_n=-15.0$. (a) The bifurcation diagram, and (b) is an enlargement of (a) near the left Hopf bifurcation point.

In addition, we can obtain an additional property by computing the bifurcation diagram with $K_n=-50$. Due to $K_n<-17.423\,57$, the created Hopf bifurcation is supercritical, as shown in Fig. 5. It can be clearly seen that the amplitude of the limit cycle is decreased by increasing the absolute value of the nonlinear control gain from Figs. 4 to 3 and 5,

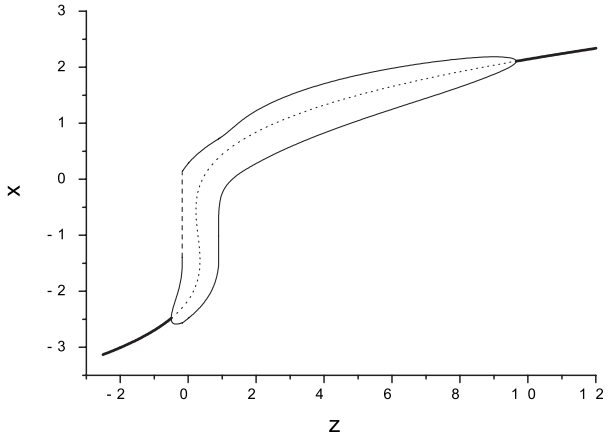

FIG. 5. The bifurcation diagram of the closed-loop system with $K_l=10.607\,43$ and $K_n=-50.0$.

which implies that one can control the amplitude of oscillation using the washout filter-aided controllers with nonlinear terms.

V. CONCLUSIONS

To sum up, from the viewpoint of bifurcation control, the type of neuronal excitability has been changed from type-I excitability to type-II excitability via a washout filter-aided dynamic feedback controller in the two-dimensional HR type model neuron. We have created a Hopf bifurcation at a desired parameter value, which is located before a SNIC bifurcation, according to the two basic critical conditions for the occurrence of the Hopf bifurcation: the eigenvalue assignment and the transversality condition. Through these two conditions we have determined the linear control gain K_l. We have applied the center manifold and normal form theory to derive the closed-form analytic expression for the bifurcation stability coefficient β_2, which is a function of the nonlinear control gain K_n. If the chosen value of K_n makes the bifurcation stability coefficient β_2 negative, the periodic solution, emanated from the created Hopf bifurcation, is stable, and then the Hopf bifurcation is supercritical. Therefore according to the criterion of the criticality of the Hopf bifurcation, we can choose an appropriate K_n to make the criticality of the created Hopf bifurcation change from subcritical to supercritical. Moreover, the application of washout filters is capable of preserving the equilibrium structure of the open-loop system as well as saving control energy. In the designed washout filter-aided dynamic feedback controller, the linear control gain underlies the critical conditions of the created Hopf bifurcation, and then determines the location of the Hopf bifurcation. The nonlinear control gain, on the other hand, governs the criticality of the Hopf bifurcation, and also regulates the amplitude of the periodic solution. Actually, the dynamic feedback controller is equivalent to a dynamically applied current, which can be injected into a given neuron, e.g., by a microelectrode. In the present paper, we have presented an approach to change the types of neuronal excitability via bifurcation control and regulate firing behavior of a model neuron. Our control method may have potential implications in suppression of undesired neural oscillations that occur in the brain.

ACKNOWLEDGMENTS

This work was supported by the National Natural Science Foundation of China under Grants No. 10502039, No. 10602041, and No. 10432010. Y.X. is grateful to the MEXT of Japan.

[1] E. M. Izhikevich, Int. J. Bifurcation Chaos Appl. Sci. Eng. **10**, 1171 (2000).
[2] J. Rinzel and G. B. Ermentrout, in *Methods in Neuronal Modelling: From Synapses to Networks*, edited by C. Koch and I. Segev (MIT, Cambridge, MA, 1998), pp. 251–291.
[3] B. S. Gutkin and G. B. Ermentrout, Neural Comput. **10**, 1047 (1998).
[4] S. Tsuji, T. Ueta, H. Kawakami, H. Fujii, and K. Aihara, Int. J. Bifurcation Chaos Appl. Sci. Eng. **17**, 985 (2007).
[5] Y. Xie, J. X. Xu, Y. M. Kang, S. J. Hu, and Y. B. Duan, Commun. Nonlinear Sci. Numer. Simul. **10**, 823 (2005).
[6] E. M. Izhikevich, Neural Networks **14**, 883 (2001).
[7] Y. Xie, J. X. Xu, and S. J. Hu, Chaos, Solitons Fractals **21**, 177 (2004).
[8] D. J. Schulz, J. Exp. Biol. **209**, 4821 (2006).
[9] J. F. Disterhoft and M. M. Oh, Aging Cell **6**, 327 (2007).
[10] H. Misonou, D. P. Mohapatra, and J. S. Trimmer, Neurotoxicology **26**, 743 (2005).
[11] R. W. Stackman, R. S. Hammond, E. Linardatos, A. Gerlach, J. Maylie, J. P. Adelman, and T. Tzounopoulos, J. Neurosci. **22**, 10163 (2002).
[12] G. Chen, J. L. Moiola, and H. O. Wang, Int. J. Bifurcation Chaos Appl. Sci. Eng. **10**, 511 (2000).
[13] H. O. Wang, D. Chen, and G. Chen, in *Proceedings of the 1998 IEEE, International Conference on Control Applications*, Trieste, Italy (IEEE Press, New York, 1998), pp. 858–862.
[14] J. Wang, L. Q. Chen, and X. Y. Fei, Chaos, Solitons Fractals **33**, 217 (2007).
[15] H. C. Lee and E. H. Abed, in *Proceedings of the American Control Conference*, Boston, MA, 1991 (American Automatic Control Council, Green Valley, AZ, 1991), pp. 206–211.
[16] A. Raman and C. D. Mote, Jr., Int. J. Non-Linear Mech. **36**, 261 (2001).
[17] H. O. Wang, E. H. Abed, and A. M. A. Hamdan, IEEE Trans. Circuits Syst., I: Fundam. Theory Appl. **41**, 294 (1994).
[18] H. O. Wang and E. H. Abed, Automatica **31**, 1213 (1995).
[19] E. H. Abed and J. H. Fu, Syst. Control Lett. **7**, 11 (1986).
[20] E. H. Abed, H. O. Wang, and R. C. Chen, Physica D **70**, 154 (1994).
[21] D. W. Berns, J. L. Moiola, and G. Chen, Automatica **34**, 1567 (1998).
[22] W. Kang, SIAM J. Control Optim. **36**, 193 (1998).
[23] M. A. Hassouneh, H. C. Lee, and E. H. Abed, in *Proceeding of the 2004 American Control Conference*, Boston, MA (IEEE Press, New York, 2004), pp. 3950–3955.
[24] G. L. Wen and D. L. Xu, Phys. Lett. A **337**, 93 (2005).
[25] J. Guckenheimer and P. Holmes, *Nonlinear Oscillations, Dynamical Systems, and Bifurcations of Vector Fields*, 5th ed. (Springer, New York, 1997), pp. 150–152.
[26] D. S. Chen, H. O. Wang, and G. Chen, IEEE Trans. Circuits Syst., I: Fundam. Theory Appl. **48**, 661 (2001).
[27] W. M. Liu, J. Math. Anal. Appl. **182**, 250 (1994).
[28] B. Ermentrout, *Simulating, Analyzing, and Animating Dynamical Systems: A Guide to XPPAUT for Researchers and Students* (SIAM, Philadelphia, PA, 2002).
[29] B. D. Hassard, N. D. Kazarinoff, and Y. H. Wan, *Theory and Application of Hopf Bifurcation*, London Mathematical Society Lecture Note Series, Vol. 41 (Cambridge University Press, Cambridge, England, 1981), pp. 86–91.